# Construction of Nonlinear Droop Relations to Optimize Islanded Microgrids Operation

Ali Elrayyah            Fatih Cingoz            Yilmaz Sozer

Electrical and Computer Engineering Department
The University of Akron
Akron, Ohio

*Abstract*- **In this paper, nonlinear droop relations are suggested to optimize the operation of islanded microgrids. By using nonlinear droop, many aspects of the microgrid operation can be optimized in addition to the inherent advantages of the droop control. In the proposed method, the droop relations are allowed to have any nonlinear shape as long as that shape satisfies certain characteristics required for the stability and proper microgrid operation. The procedure of constructing the nonlinear droop relations that minimize the operating cost of the microgrid and share the reactive power effectively among the sources is investigated and explained in detail. The selected droop structure is a combination of integer and fractional power functions whose parameters are selected using two-stage particle swarm optimization algorithm. The effectiveness of the proposed method is verified through simulation and experimental studies.**

*Keyword: Nonlinear Droop, power sharing, particle swarm optimization*

## I. INTRODUCTION

Nowadays, there is an accelerated trend to modernize power systems by including more sources in the distribution voltage level and adding intelligence to the devices and their controllers [1]. The concepts of microgrid came to be an outcome of this modernization whereby many technical, economical and environmental benefits can be harnessed. The microgrid is an independent low or medium voltage power network that combine distributed generators, energy storages and loads. The microgrid can be operated in three modes: 1) grid-connected, 2) islanded or 3) transition mode [2-4].

The droop control is accepted widely as a suitable candidate to control the sources in islanded microgrids [5], [6]. In the conventional droop control, the frequency ($f_i$) and the output voltage ($V_{out,i}$) for the $i^{th}$ source are adjusted according to the following relations:

$$f_i = f_{ref} - K_{p,i}P_i \qquad (1)$$

$$V_{out,i} = V_{ref,i} - K_{q,i}Q_i \qquad (2)$$

The variables $f_{ref}, V_{ref,i}$, $P_i$ and $Q_i$ are the reference frequency, reference voltage, real and reactive power, respectively. The parameters $K_{p,i}$ and $K_{q,i}$ are the droop controllers coefficients and based on the values of these parameters, the real and reactive power needed by the load are shared among the sources [7]. The relations in Eqn. 1 and 2 are based on the fact that real and reactive power of the sources having and inductive coupling with the microgrid are given by:

$$P_i = \frac{V_{out,i}V_\mu \sin \delta}{X_{L_i}} \qquad (3)$$

$$Q_i \approx \frac{V_{out,i}(V_{out,i} - V_\mu)}{X_{L_i}} \qquad (4)$$

where $V_\mu$ is the microgrid voltage at the coupling point of the $i^{th}$ source, $X_{L_i}$ is its coupling impedance which represents the inductor of the source filter and $\delta$ is the phase difference between the source and the microgrid. From these relations the real power can be adjusted independently from the reactive power by adjusting the former through changing the angle $\delta$ and the later by varying the voltage amplitude $V_{out}$.

The droop control characteristics can be explained as below

- Since the frequency in the microgrid is a universal signal, the real power between the sources is shared accurately according to the ratios of $K_{p,i}$ of different sources.
- Since the voltage is a local signal, the reactive power sharing is affected by the proximity of the source to the load in addition to the value of $K_{q,i}$ [8].
- As it allows the sources to share the load and regulate the voltage, the droop control satisfies the required reliability for islanded microgrid operation [9, 10].

In this paper, optimized nonlinear droop control relations along with their construction method to improve and enhance microgrids operation are proposed. In addition to the tasks mentioned above, the droop controllers in this paper are constructed to achieve operation management and resource optimization. The need to include the optimization factor in the droop operation is justified first. Then, a framework to develop droop relations for that task is presented. The main idea is to introduce a generalized formulation of the droop relations as follows:

$$f_i = f_{ref} - F_{drp,i}(P_i) \qquad (5)$$

$$V_{out,i} = V_{ref,i} - V_{drp,i}(P_i, Q_i) \qquad (6)$$

The functions $F_{drp,i}(.)$ and $V_{drp,i}(.)$ are arbitrary nonlinear functions which have to be selected properly to achieve certain optimization objectives. Different objectives can be considered such as loss minimization, and voltage

regulation. The proposed method can be utilized to tackle different objectives; however, only two objectives are selected in this paper. These objectives are: fuel consumption minimization and the reactive power sharing error minimization. The first objective is to minimize the operating cost of the sources while satisfying the power demand under all loading conditions. The second objective aims to share the reactive power among the sources based on their power ratings. Effective reactive power sharing is important since it distributes the thermal stress evenly among the sources avoiding early failure that may be caused by overloading [11].

Optimizing microgrids operation can be achieved using supervisory control where a centralized optimization algorithm needs to be executed in the central controller and then the power to be produced by every source could be commanded using communication system. When compared with the nonlinear droop method, the supervisory control is more costly and less reliable. On the other hand, the droop control, including the proposed nonlinear droop, is very robust and reliable such that it provides its function even when some sources fail. However, the advantage of the two techniques can be combined in one system where the central controller can adjust the parameters of the nonlinear droop relations of the individual controllers whenever there is a change in the power system structure such that any update in the power system could be addressed without affecting the reliability of the system.

The rest of the paper is organized as follows. Section II shows the procedure of constructing the nonlinear functions for the droop relations. These nonlinear functions need to satisfy certain characteristics to maintain the stability of the microgrid. This procedure is used in Section III to develop set of nonlinear droop relations that optimizes the microgrid operation. The optimization mentioned in Section III is based on using particle swarm optimization in two stages. A stability analysis of nonlinear droop based microgrids is presented in Section IV. The simulation and experimental results are provided in Section V and VI, respectively to verify the effectiveness of the proposed method. Finally the paper is concluded in Section VII.

## II. SELECTION OF NONLINEAR DROOP RELATIONS

Two objectives are set to be satisfied in this paper, these objectives are:

- Minimizing the cost of the microgrid operation by sharing the real power effectively among the sources.
- Optimizing the reactive power sharing to achieve uniform distribution across all sources.

The operating cost in power systems depends on the fuel consumption by the sources. The amount of the consumed fuel depends on the real power produced by the sources in the microgrid. Usually, the operating cost of each source does not vary linearly with the amount of the power production. In fact, there are some operating regions that have relatively low operating cost due to the relatively higher efficiency on these operating regions [12]. Therefore, the operating cost of the sources exhibits nonlinear behavior. To minimize the operating cost, nonlinear droop relations can be developed to take this nonlinearity into consideration.

Microgrid operating cost reduction has higher importance than other objectives such as reactive power sharing. Therefore, this objective is better to be linked with the frequency droop relation. The frequency droop relation shown in Eqn. 1 makes the real power to be shared precisely between the sources in proportion to the setting of their droop parameters. Therefore, the nonlinear function $F_{drp,i}(.)$ in Eqn. 5 is considered to be function of $P_i$ only to ensure the accurate sharing. On the other hand, $V_{drp,i}(.)$ in Eqn. 6, which affects the reactive power sharing, is taken as a function of both $Q_i$ and $P_i$ for the sake of generalizing the voltage droop relation.

Not all functions can be used to represent $F_{drp,i}(.)$ and $V_{drp,i}(.)$, rather there are certain characteristics that need to be satisfied by the nonlinear function before it can be used to represent $F_{drp,i}(.)$ or $V_{drp,i}(.)$. These characteristics are:

- They should possess high degree of nonlinearity to provide the required flexibility for optimizing all types of cost functions for the sources.
- They should have monotonic relations such that every frequency drop in $F_{drp,i}(.)$ can be achieved by single value of $P_i$. This is required to achieve single solution for the optimization problem at every loading condition.
- The slopes $\frac{\partial F_{freq}}{\partial P_i}, \frac{\partial F_{freq}}{\partial Q_i}, \frac{\partial F_{vol}}{\partial Q_i}$ and $\frac{\partial F_{vol}}{\partial P_i}$ should ensure the microgrid stability. To establish negative feedback in the droop relation, the following relations need to be satisfied: $\frac{\partial F_{freq}}{\partial P_i} > 0$ and $\frac{\partial F_{vol}}{\partial Q_i} > 0$.

Since the number of available nonlinear functions is infinite, constructing the appropriate nonlinear functions to be used for $F_{drp,i}(.)$ and $V_{drp,i}(.)$ could be challenging. A reasonable approach is to represent the nonlinear functions as the combination of a number components or building blocks, which are basic nonlinear functions. Then, the complexity of $F_{drp,i}(.)$ and $V_{drp,i}(.)$ can be increased or decreased by adjusting the number and the weights of these components as needed. This approach helps in optimizing the selection of the droop relations as what will be shown in the next section.

The structure of the function $F_{drp,i}$ in this paper is considered as

$$F_{drp,i}(P_i) = \sum_{j=1}^{N} K_{fphi,j} P_{n,i}^j + K_{fpli,j} P_{n,i}^{1/j} \qquad (7)$$

$$P_{n,i} = P_i / P_{iRated}$$

The variable $P_{iRated}$ and $P_{n,i}$ are the rated and per unit power of the $i^{th}$ source, respectively. The parameter $j$ is the summation variable that specifies the power of each component. In Eqn. 7, the function $F_{drp,i}(.)$ is taken as the combination of integer and fractional power functions whose coefficients ($K_{fphi,j}$ and $K_{fpli,j}$) are all positive. When the coefficient of $F_{drp,i}(.)$ are positive, the value $\partial F_{drp,i}/\partial P_i$ will be non-negative since $P_{n,i}$ is positive. Normal polynomials can be used to construct nonlinear droop relations, but for them to construct any required nonlinear droop relations, some coefficients might become negative. When the coefficients are allowed to take negative values, the condition of $\partial F_{drp,i}/\partial P_i > 0$ has to be checked all the time. This checking lengthens and complicates the constructing process of the functions. Through the use of a mixture of polynomial and fractional-exponents polynomial, merely positive coefficients are needed for the droop relation without losing the flexibility of shaping general nonlinear curves. Moreover, the condition $\partial F_{drp,i}/\partial P_i > 0$ is always satisfied.

Figure 1 shows the plot of the components $P_{i,n}^j$ and $P_{n,i}^{1/j}$ of $F_{drp,i}$. Clearly, with the proper selection of the parameters $K_{fphi,j}$ and $K_{fpli,j}$, various nonlinear waveforms can be constructed for $F_{drp,i}$. For example, as Fig. 2 shows three nonlinear droop relations are formulated, which are

$$F_{drp,1} = 0.04\, P_{n,i} + 0.05\, P_{n,i}^{\frac{1}{7}} + 0.01 P_{n,i}^8,$$

$$F_{drp,2} = 0.01\, P_{n,i} + 0.03\, P_{n,i}^{\frac{1}{3}} + 0.06 P_{n,i}^8, \text{ and}$$

$$F_{drp,3} = 0.1\, P_{n,i}.$$
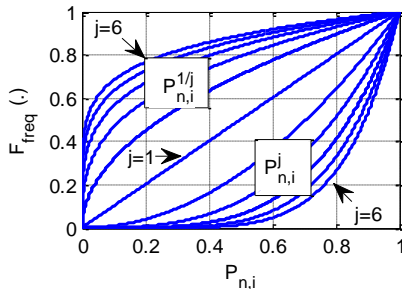


Figure 1 Components of $F_{drp,i}$.
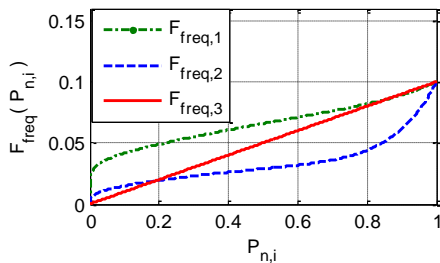


Figure 2. Examples of $F_{drp,i}$ relations.

Similar to the construction of the function $F_{drp,i}(.)$, the function $V_{drp,i}(.)$ can be selected as

$$V_{drp,i} = V_{drp,ip}(P_i) + V_{drp,iq}(Q_i) \qquad (8)$$

where

$$V_{drp,ip}(P_i) = \sum_{j=1}^{N} \left( K_{vphi,j} P_{i,n}^j + K_{vpli,j} P_{i,n}^{1/j} \right)$$

$$V_{drp,iq}(Q_i) = \sum_{j=1}^{N} \left( K_{vqhi,j} Q_{i,n}^j + K_{vqli,j} Q_{i,n}^{1/j} \right)$$

where $P_{n,i}$ and $Q_{n,i}$ are the per unit value for the real and reactive power, respectively.

### III. CONSTRUCTION OF NONLINEAR DROOP RELATIONS

The optimal selection of the parameters $K_{fphi,j}$, $K_{fpli,j}$, $K_{vphi,j}$, $K_{vqhi,j}$, $K_{vpli,j}$, and $K_{vqli,j}$ for $j = 1, 2, \ldots, N$ in Eqn. 7 and 8 has to be performed to optimize microgrids operation. The problem in hand can be formulated as to find the values of

$$V_{refi}, K_{fphi,j}, K_{fpli,j}, K_{vphi,j}, K_{vpli,j}, K_{vqhi,j}, K_{vqli,j}|_{j=1,\ldots,N\,;\,i=1,2,\ldots,N_s}$$

that minimize

$$\sum \{ C_1(P_1, \ldots, P_{N_s}) + C_2(Q_1, \ldots, Q_{N_s}) \} \qquad (9)$$

where $C_1(P_1, \ldots, P_{N_s})$ is for the operating cost and $C_2(Q_1, \ldots, Q_{N_s})$ is for the reactive power sharing cost. The summation in the problem is taken to consider different loading conditions where $N$ is the number of the terms in the droop nonlinear functions and $N_s$ is the number of sources in the microgrid, respectively. The voltages $V_{refi}, i = 1, 2, \ldots N_s$ are included in the optimization problem as they affect the reactive power sharing.

The problem is very complex and it could be very difficult if not impossible to be solved analytically. However, heuristic techniques can be used effectively to solve the optimization problem in Eqn. 9. One of the best heuristic optimization techniques for this kind of problems is the particle swarm optimization (PSO) [13, 14]. In PSO, a number of particles are selected and each particle represents one solution to the problem i. e. specific selection for parameters;

$$V_{refi}, K_{fphi,j}, K_{fpli,j}, K_{vphi,j}, K_{vpli,j}, K_{vqhi,j}, K_{vqli,j}|_{j=1,\ldots,N\,;i=1,\ldots,N_s}.$$

Initially, random selection is taken for the particles and then the cost of each particle is calculated. Based on the smallest cost among all particles and the history of the local cost of each particle, the parameters of each particle are modified. The algorithm continues for a number of iterations and the particle whose parameters give the minimum cost is taken as the optimum solution [15, 16].
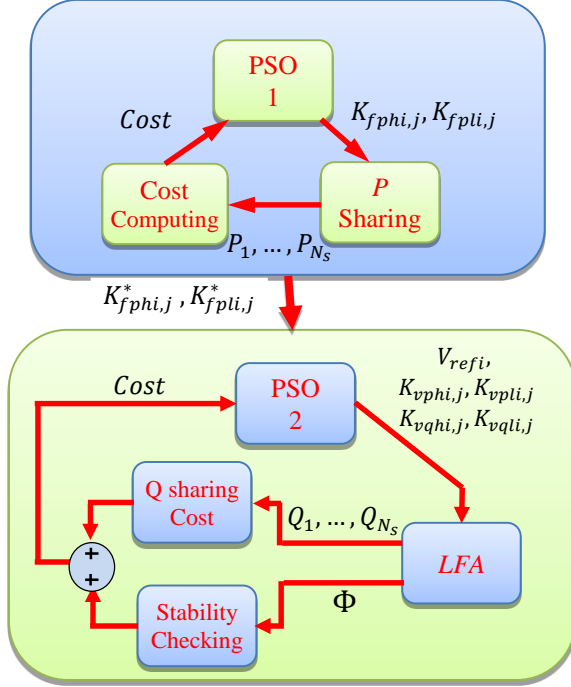
Figure 3. Proposed optimization stages.

The proposed optimization method is described in Fig. 3. The problem is solved in two stages since the real power and the reactive power can be adjusted independently as indicated in Eqn. 2 and 3. First, since the frequency is a universal signal and accordingly the real power sharing is independent from the microgrid topology, the selection of the functions $F_{drp,i}$ is made. In this stage, the following optimization problem is solved:

$$\min_{K_{fphi,j}, K_{fpli,j}|_{j=1,\dots,N,i=1,2,\dots,N_s}} F_P(P_1, P_2, \cdots, P_{N_s}) \qquad (10)$$

$$F_p(P_1, P_2, \cdots, P_{N_s})$$
$$= \sum_{n=1}^{N_{L.C.}} \{C_{P1}(P_{1,n}) + C_{P2}(P_{2,n}) + \cdots + C_{PN_s}(P_{N_s,n})\}$$

with the constrains

$$F_{drp,1}(P_{1,n}) = F_{drp,2}(P_{2,n}) = \cdots = F_{drp,N_s}(P_{N_s,n}) \qquad (11)$$
$$P_{1,n} + P_{2,n} + \cdots + P_{N_s,n} = P_{total,n} \qquad (12)$$

where and $P_{i,n}$ is the output power of the $i^{th}$ source for the $n^{th}$ loading condition and $C_{Px}(P_{x,n})$ is the fuel cost of producing the amount of power $P_{x,n}$ by the $x^{th}$ source. $P_{total,n}$ is the total load at the $n^{th}$ steps and its value changes from the smallest to the highest condition. In each case, the cost is calculated and summed in Eqn. 10. Accordingly, the cost under all loading conditions ($N_{L.C.}$) will be minimized by the proper selection of the parameters $K_{fphi,j}$ and $K_{fpli,j}$.

The second stage is to select the parameters $V_{refi}, K_{vphi,j}, K_{vpli,j}, K_{vqhi,j}, K_{vql,j}|_{j=1,\dots,N,i=1,2,\dots,N_s}$ such that the reactive power sharing is performed effectively. For explanation purposes, let the output of the stability checking

block be zero. The reactive power generated by the sources depends on the microgrid topology, the amount of the loads and the positions of the sources and loads in the microgrid. The power produced by every source can be determined using the load flow analysis (LFA) for microgrids operation [17-19]. In LFA performed for microgrids, the phase of every sources is determined from the frequency droop relation while the voltage is obtained from the voltage droop relations. Then, the voltages and phases of all sources are used along with the microgrid topology and the connected loads to determine the power produced by every source.

To determine the proper selection for nonlinear relations for the voltage droop, PSO can be used to find the values for the parameters $V_{refi}, K_{vphi,j}, K_{vpli,j}, K_{vqhi,j}$ and $K_{vql,j}$ that minimizes the error in the reactive power sharing. The setting of the frequency droop relation are obtained from stage 1, as shown in Fig. 3. Then, selections are made for the parameters of the voltage droop relations using the PSO. The LFA is then performed for the microgrid under different loading conditions. In each case, the reactive power sharing cost due to the deviation from the equal sharing is obtained. Based on the cost obtained for each one of the selected particles, the PSO algorithm performs new selection for the considered particles. As stated before, the algorithm will compute for a number of iterations and the set of parameters that yields the minimum cost is taken as the optimum solution.

The PSO is a time consuming algorithm, however it does not have to be implemented in real time. As explained before, the optimization can be performed whenever there is a change in the nature and number of connected sources and the new settings for the droop controllers can be send to the individual sources. After performing the calculations of the two stages shown in Fig. 3, the proper values for the nonlinear droop relations are obtained. These values can be used to manage the optimal operation for the sources in the microgrid.

IV. STABILITY OF MICROGRIDS WITH NONLINEAR DROOP CONTROL

One important aspect that needs to be investigated for the microgrids with nonlinear droop is its stability. Despite the fact that the nonlinear droop relations were formulated in such a way that the unstable operation of the sources is avoided, a mathematical tool needs to be develop to ensure the stable operation of the entire microgrid. Consider the case of a microgrid that combines $N_s$ sources. The phases of the sources are given by:

$$\dot{\delta}_i = f_{ref} - F_{drp,i}(P_i) \qquad (13)$$

where $\delta_i$, $F_{drp,i}(.)$ and $P_i$ are the phase, frequency droop relation and the power of the $i^{th}$ source, respectively i=1, 2, …, $N_s$. The reference frequency $f_{ref}$ is a fixed value used for all sources. As shown in [20], the phase of any one of the

sources can be taken as reference. Let that source be the $k^{th}$ source, the phase of all sources can be written as:

$$\dot{\delta}_{i,k} = \left(f_{ref} - F_{drp,i}(P_i)\right) - \left(f_{ref} - F_{drp,k}(P_k)\right)$$
$$= F_{drp,k}(P_k) - F_{drp,i}(P_i) \quad (14)$$

where $\delta_{i,k}$ is the phase of the $i^{th}$ source when the phase of the $k^{th}$ source is taken as a reference. The relation in Eqn. 14 is nonlinear, after linearization it becomes:

$$\dot{\tilde{\delta}}_{i,k} = \tilde{p}_k \frac{\partial F_{drp,k}(P_k)}{\partial P_k}|_{P_k=\bar{P}_k} - \tilde{p}_i \frac{\partial F_{drp,i}(P_i)}{\partial P_i}|_{P_i=\bar{P}_i} \quad (15)$$

where $\tilde{z}$ is the perturbation in the variable $z$ and $\bar{Z}$ is its value in the operating point. Similar to the phase relation, the voltage of $i^{th}$ source is given by:

$$V_{out,i} = V_{ref,i} - V_{drp,i}(P_i, Q_i) \quad (16)$$

After linearization, Eqn. 16 becomes:

$$\tilde{v}_{out,i} = -\tilde{p}_i \frac{\partial V_{drp,i}(P_i,Q_i)}{\partial P_i}|_{\substack{Q_i=\bar{Q}_i \\ P_i=\bar{P}_i}} - \tilde{q}_i \frac{\partial V_{drp,i}(P_i,Q_i)}{\partial Q_i}|_{\substack{Q_i=\bar{Q}_i \\ P_i=\bar{P}_i}} \quad (17)$$

The real and reactive power used in Eqn. 14 and 17 are filtered versions of the instantaneous values of the power components $P_{int,t}$ and $Q_{int,t}$. The used filter has cutoff frequency, $w_f$. Then, the filtered power is given by:

$$P_i = \frac{w_f}{s+w_f} P_{int,i} \rightarrow \dot{P}_i = w_f\left(P_{int,i} - P_i\right) \quad (18)$$

In term of small signal model, Eqn. 18 becomes:
$$\dot{\tilde{p}}_i = w_f\left(\tilde{p}_{int,i} - \tilde{p}_i\right) \quad (19)$$
Similarly, the reactive power is given by:
$$\dot{\tilde{q}}_i = w_f\left(\tilde{q}_{int,i} - \tilde{q}_i\right) \quad (20)$$
Equations 13-18 can be combined in the following set of linear equations:

$$\dot{\tilde{x}} = A\tilde{x} + G\tilde{\omega} \quad (21)$$
$$\tilde{x} = \begin{bmatrix} \tilde{p}_1 & \tilde{q}_1 & \tilde{\delta}_{1,k} & \dots & \tilde{p}_i & \tilde{q}_i & \tilde{\delta}_{i,k} & \dots \end{bmatrix} \quad (22)$$
$$\tilde{\omega} = \begin{bmatrix} \tilde{p}_{int,1} & \tilde{q}_{int,1} & \dots & \tilde{p}_{int,i} & \tilde{q}_{int,i} & \dots \end{bmatrix} \quad (23)$$
From the voltage $V_{out,i}$ and the phase $\delta_{i,k}$, the value of $P_{int,i}$ and $Q_{int,i}$ can be obtained from the LFA tool which is given by:
$$\Psi\left( \dots, V_{out,i}, \delta_{i,k}, P_{int,i}, Q_{int,i}, \dots \right) = 0 \quad (24)$$
where, $\Psi(.)$ is the set of relations used in the LFA of the microgrid under consideration. After linearization, Eqn. 24 can be written as:
$$\frac{\partial \Psi}{\partial x}\tilde{x} + \frac{\partial \Psi}{\partial \omega}\tilde{\omega} = 0 \rightarrow \tilde{\omega} = -\left(\frac{\partial \Psi}{\partial \omega}\right)^{-1}\frac{\partial \Psi}{\partial x}\tilde{x} \quad (25)$$

Then, Eqn. 25 can be combined with Eqn. 21 to yield the following linearized model for the microgrid,

$$\dot{\tilde{x}} = A\tilde{x} - G\left(\frac{\partial \Psi}{\partial \omega}\right)^{-1}\frac{\partial \Psi}{\partial x}\tilde{x} = \Phi\tilde{x} \quad (26)$$

where

$$\Phi = \left(A - G\left(\frac{\partial \Psi}{\partial \omega}\right)^{-1}\frac{\partial \Psi}{\partial x}\right) \quad (27)$$

The eigenvalues of the matrix $\Phi$ can be obtained to check the stability of the microgrid system. Clearly, the matrix $\Phi$ will have different sets of eigenvalues for every loading condition. There are two conditions that need to be satisfied to ensure the stability of the microgrid. These conditions are:

a. All eigenvalues for $\Phi$ should be negative for all loading conditions

b. The change in the microgrid loading condition should be relatively in frequent.

These two conditions are the necessary conditions for the stability of a system that switches between different modes of operation [21]. For microgrids, the changes in the loading condition that cover normal and highly stressing loading are considered as changes in the microgrid mode of operation since it changes the parameters in the matrix $\Phi$. This consideration allows the stability of microgrids to be checked using the well-established method of switched systems.

The second condition is usually satisfied in microgrids since the loads do not change very frequently. The times between load variations in microgrid is in seconds if not longer. This duration is much longer than the response time of the dynamics in Eqn. 27 [22, 23].

To satisfy the first condition, the eigenvalues for the matrix $\Phi$ can be checked while constructing the nonlinear droop functions. As shown in Fig. 3, the eigenvalues of $\Phi$ under all loading condition is checked for every selection of the nonlinear droop coefficients. In case of a particle producing stable eigenvalues, this particle is accepted and the stability checking block adds zero to the cost calculated by the reactive power droop relation. On the other hand, for a particle that produces an unstable case, the stability checking block adds a very large number to the calculated cost to discard this particle from the possible solutions. Accordingly, the selected nonlinear droop functions automatically ensures the stable operation in the microgrid.

Since the changes in the nonlinear droop relations are needed only when there is a change in the number of connected sources, the stability should be checked also whenever a new set of nonlinear relations is constructed. To ensure the stable operation for this new set, different loading conditions including the stressing loading condition should be checked. In this way, the stable operation can be guaranteed under all loading conditions.

## V.  SIMULATION RESULTS
The microgrid depicted in Fig. 4 is performed in this simulation section to validate the proposed nonlinear droop formulation and optimization method.
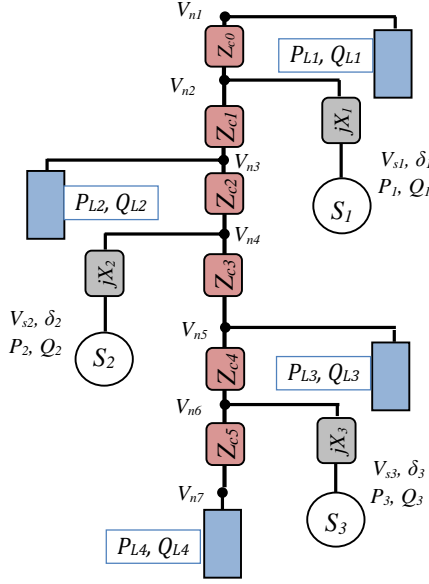
Figure 4. Considered microgrid topology for the simulation study.

The parameters of the microgrid are shown in Table 1. To select the parameters $K_{fphi,j}$ and $K_{fpli,j}$ for the real power sharing, the cost of power production of each one of the three sources is assumed as those shown in Fig. 5. A general cost unit is taken as dimensionless value is considered to be used for the optimization problem.

Table 1. Parameters of the microgrid in Fig. 4.

| $Z_0$= 0+j0.02 | $Z_3$=0+j0.026 | $jX_{L1}$=j0.2639 |
|---|---|---|
| $Z_1$ = 0+j0.04 | $Z_4$=0+j0.023 | $jX_{L2}$=j 0.1885 |
| $Z_2$= 0+j0.034 | $Z_5$ = 0+j0.03 | $jX_{L3}$=j 0.1508 |
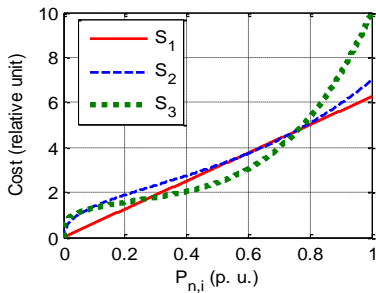


Figure 5. Real power costs of the sources

After solving the optimization problem in Eqn. 10 using PSO that has 50 particles and run for 50 iteration, the functions $F_{drp,1}$, $F_{drp,2}$ and $F_{drp,3}$ are found as shown in Fig. 6 and their formulae are listed in Table 2.

Table 2. Frequency droop relations as Stage 1 output.

| $P_{n,1} = P_1/1200$ | $P_{n,2} = P_2/1400$ |
|---|---|
| $P_{n,3} = P_3/1400$ | $F_{drp,1} = 0.1 P_{n,1}$ |
| $F_{drp,2} = 0.1/3(P_{n,2} + P_{n,2}^2 + P_{n,2}^{0.5})$ | |
| $F_{drp,3} = 0.1/5.5\left(P_{n,3}^4 + P_{n,3}^7 + \frac{1}{2}P_{n,3}^8 + P_{n,3}^{1/5} + P_{n,3}^{1/6} + P_{n,3}^{1/9}\right)$ | |
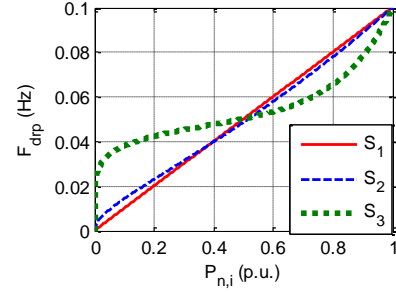


Figure 6. $F_{drp,1}$, $F_{drp,2}$ and $F_{drp,3}$ obtained from the PSO stage 1.

To evaluate the gain obtained by this optimization method, the power production cost obtained by the proposed method is compared with that of the normal linear droop where the three sources are operated to produce the same amount of power. The comparison is shown in Fig. 7. Clearly, the proposed method reduced the cost significantly when it is compared with linear droop relation of equal sharing.
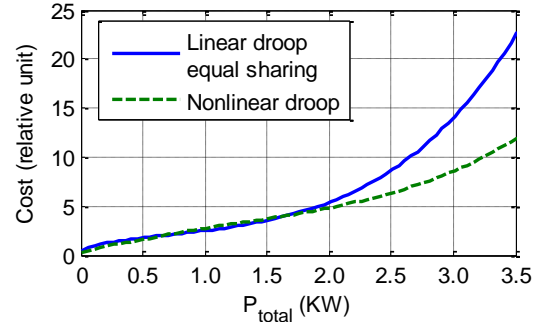


Figure 7. Comparison between the real power production cost in the optimized nonlinear droop and the conventional one.

In the second stage, the optimized frequency droop relations were used. By considering 16 loading conditions that covers the possible range of the load, the parameters
$$V_{refj}, K_{fph,j}, K_{fpl,j}, K_{vph,j}, K_{vpl,j}, K_{vqh,j}, K_{vql,j}|_{j=1,...,N}$$
were obtained using the PSO. Figure 8 shows the function $V_{drp}$ as two curves, one for the reactive power while the other is for the real power. The values of $V_{ref1}$, $V_{ref2}$ and $V_{ref3}$ are found to be 123.2, 122 and 121.7, respectively. The optimization method selected positive signs of the real power term in $V_{drop}$ such that it increases the source output voltage as the real power increases. This helps in regulating the load voltage as it compensates for the voltage drop in the coupling lines.
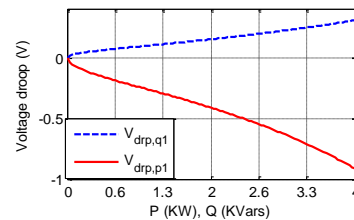


Fig. 8(a)
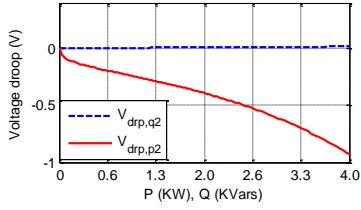
Fig. 8(b)
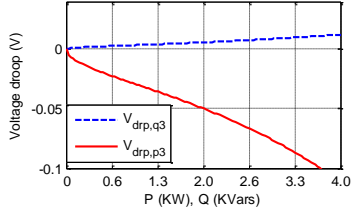
Fig. 8(c)

Figure 8. The nonlinear voltage droop function produced by stage 2 in the PSO for (a) source 1 (b) source 2 and (c) source 3.
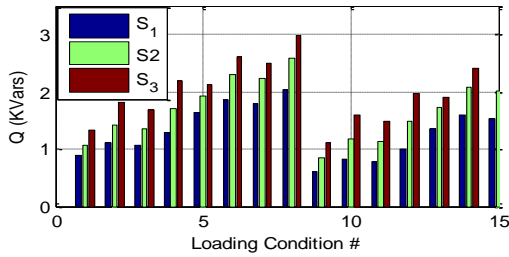
Figure 9. Reactive power sharing amongthe three sources using the conventional linear droop.
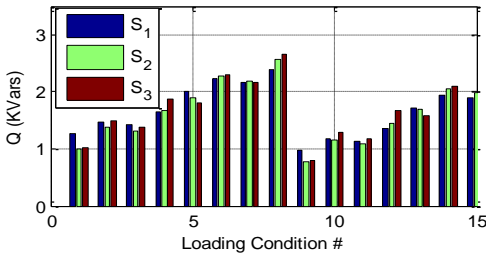
Figure 10. Reactive power sharing amongthe three sources using the proposed nonlinear droop.

To evaluate the performance of the proposed method, the conventional linear voltage droop was considered for the three sources where the objective is to share the reactive power equally among the three sources. Figure 9 shows the linear droop load reactive power distribution among the sources. Clearly, the source S1 has the least stress among the three sources for all loading conditions as the conventional voltage droop relations do not take into account the location of sources and its proximity to the load. For example, according to the conventional droop, the source S1 placed at the edge of the microgrid in Fig. 4 contributes much less reactive power than the other sources. However, as Fig. 10 shows, the proposed nonlinear droop optimization problem considers the position of the source while selecting the droop parameters. Clearly, the proposed

method produces better reactive power sharing which is close to a uniform sharing in contrast with the conventional linear droop. These results verify the effectiveness of the method proposed in this paper.

To check the stability of the microgrid, Eigen values of the Φ were obtained. The locus of two of Eigen values as the load changes are shown in Fig. 11. This Eigen values reflect the response time of the power production in the microgrid. As the load increases some of the dynamics become slower while others show lower damping as shown in Fig. 12. Nevertheless, the microgrid is proven to stable under all these loading conditions. Therefore, the developed techniques can be used to analyze the microgrid dynamics and check its stability.
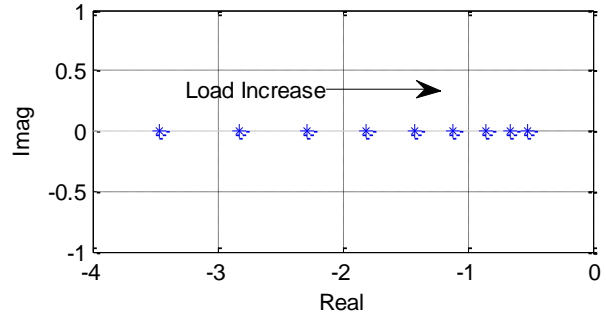
a.    Stable root with slower dynamics as the load increases
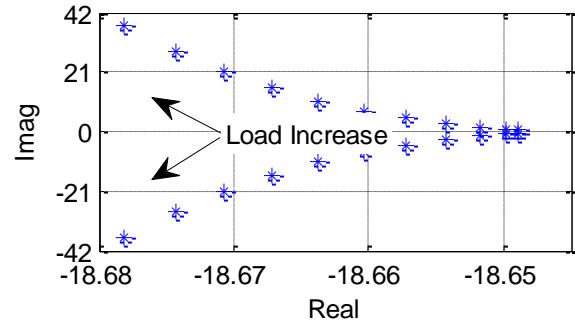
b.    Stable root with slower less damping as the load increases

Figure 11. Two of the matrix Φ Eigen values as the loading condition changes.

To compare the response of the linear droop control with that of the nonlinear droop control, consider the curves in Fig. 12 and 13. In Fig. 12, the real power productions and the frequencies of the three sources are shown for the linear droop case where the three sources use the same droop parameters. The three sources in this case share the load demand equally. The load is allowed to vary such that the dynamical response can be analyzed. The load takes the values 2.85 kW from 0 to 2.5 seconds, 3.6 kW from 2.5 to 7.5 seconds and 4.7 kW after 7.5 seconds. Figure 12(b) also shows that the frequency of the three sources always have the same value and similar dynamical responses.

(a) Real power produced by $S_1$, $S_2$ and $S_3$.



(b) Frequency of $S_1$, $S_2$ and $S_3$.
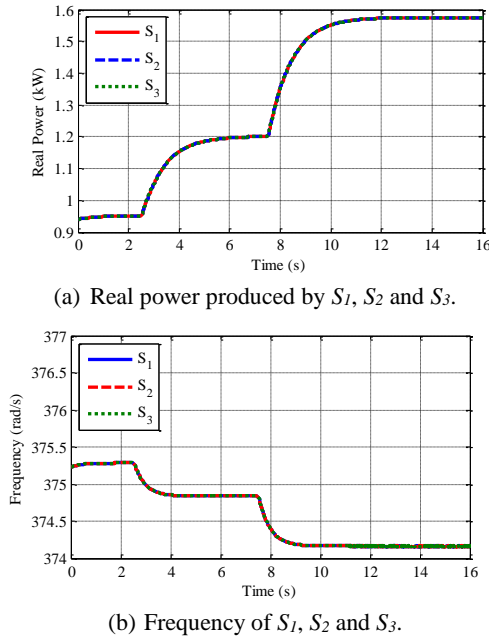
Figure 12. Simulation results for the real power and frequency of the microgrid sources using linear droop relations.

Figure 13 on the other hand shows the power productions and the frequencies of the three sources when they are controlled using the nonlinear droop relations. Unlike the linear droop case, the three sources produce different amounts of power and as the load changes, the power sharing among them varies. From 0 to 5 seconds, each of source 1 and 2 produces more power than source 3, but as the load increases at 5 seconds, the production of source 3 exceeds that of source 1 and 2. By observing the cost curves of the three sources shown in Fig. 5, this behavior will be found to be the preferred one. Before 5 seconds, the load value is distributed mostly over the low cost regions of source 1 and 3 while the source 3 was less loaded as it has high cost. When the load increases, however, it become inapplicable to maintain the low cost operation in source 1 and 2 as their operating costs increase. On the other hand, the operating cost of source 3 decreases with the load increase at that moment. Therefore, the nonlinear droop relation causes the power production of source 1 and 2 to become less than that of source 3 and thus reducing the operation cost. Figure 13(b) shows that the

three sources operate at the same frequency despite the variations in the load sharing, which is obtained from using the nonlinear droop relations shown in Fig. 6.



(a) Real power produced by $S_1$, $S_2$ and $S_3$.



(b) Frequency of $S_1$, $S_2$ and $S_3$.
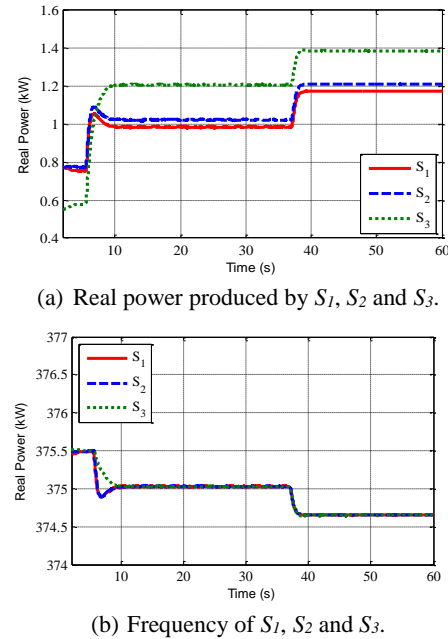
Figure 13. Simulation results for the real power and frequency of the microgrid sources using nonlinear droop relations.

## V.    EXPERIMENTAL RESULTS

In this section, the proposed nonlinear droop method is verified experimentally. Three inverters were used for the three sources. The inverters were controlled using TMS320f28335 digital signal processor (DSP) and NHresearch 4200 programmable AC loads were used to represent the various loads in the microgrid. The same microgrid topology shown in Fig. 4 with the same parameters was implemented for the experimental testing. The experimental microgrid setup is shown in Fig. 14.

The waveforms of the currents of the three sources and the voltage at one of node voltages are shown in Fig. 15. From Fig. 15 the waveforms are proper and voltage in the load node is well-regulated.
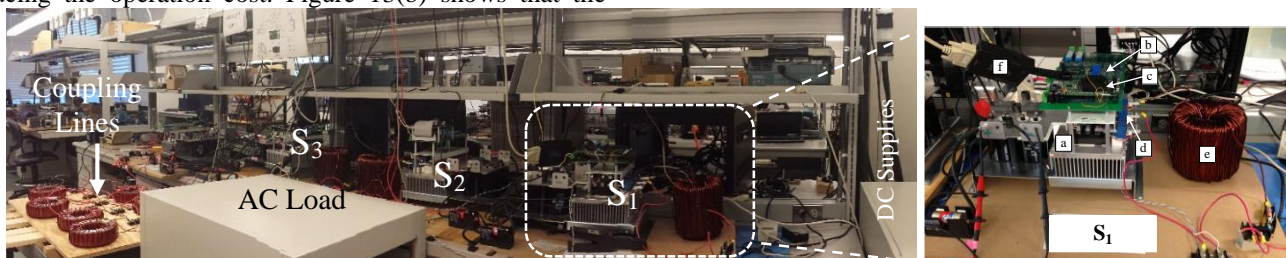


Figure 14. Experimental setup for the considered microgrid. $S_1$ components:  (a) Inverter unit, (b) Interfacing control board, (c) DSP board, (d) Current sensor, (e) L-filter, and (f) JTAG Emulator.
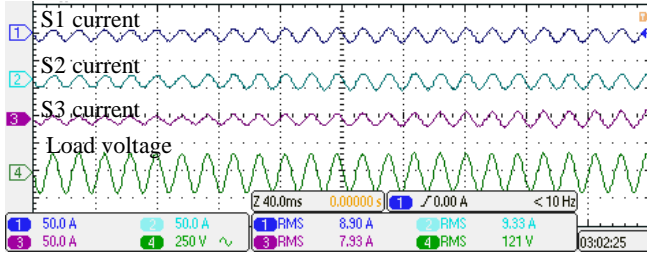
Figure 15. Current and voltage waveforms for nonlinear droop based sources in the microgrid of Fig. 4.

Figure 16 shows the power sharing among the three sources using the conventional linear droop with equal sharing. When, compared with Fig. 12, the experimental results are found to match exactly with the one provided by the simulation. Then, both the power produced by the sources and their frequency verified the accuracy of the implemented experiment.
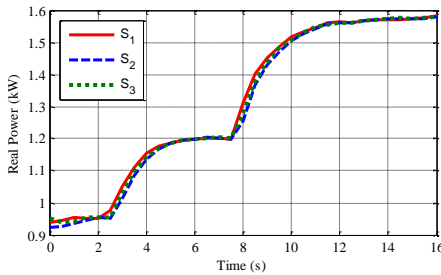


(a) Real power produced by $S_1$, $S_2$ and $S_3$
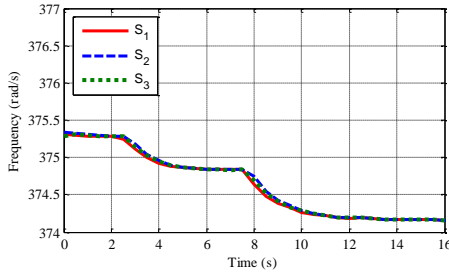


(b)Frequency of $S_1$, $S_2$ and $S_3$

Figure 16. Simulation results for the real power and frequency of the microgrid sources using nonlinear droop relations.

In another experiment, the nonlinear droop relation shown in Fig. 6 were implemented in look-up tables (LUT) that were stored in the DSP. The power produced by the sources are then measured and normalized to be used as input to the LUT whose output represents the required value to be implemented in the frequency droop relation. Figure 17 shows the power produced by the three sources and their frequencies. Clearly, these results match very accurately the one obtained by simulation and shown in Fig. 13. Figure 17 shows that, the power sharing among the three sources is not fixed but it varies with the loading condition in a way that minimizes the operation cost. The frequency response in Fig. 17(b) verifies that the dynamical response of the frequency in the microgrid is stable and smooth.

Accordingly, the proposed nonlinear droop method is verified experimentally to minimize the operation cost while maintaining the smooth and stable operation in the microgrid.
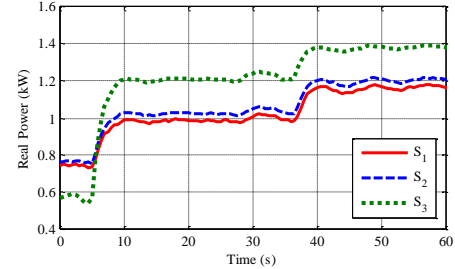


(a) Real power produced by $S_1$, $S_2$ and $S_3$
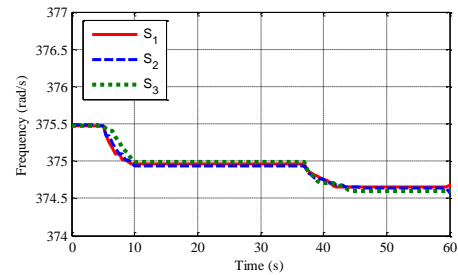


(b) Frequency of $S_1$, $S_2$ and $S_3$

Figure 17. Simulation results for the real power and frequency of the microgrid sources using nonlinear droop relations.

## VI. CONCLUSION

In this paper, a method is proposed to optimize the operation of islanded microgrid using general nonlinear relations for the droop control. With the proper selection of the droop relations, the voltage and frequency in the microgrid can be stabilized and regulated. Moreover, the same droop relations can be used to optimize the microgrid operation by considering factors such as fuel cost, system losses and voltage regulation while developing these relations. To add flexibility in the selection of the droop relations, they are considered in this paper to be arbitrary nonlinear relations. After the required characteristics of the acceptable droop relations, a mixture of normal polynomial and polynomial with fractional-exponents is found to be feasible and flexible enough to produce any required nonlinear droop relation. The parameters of those polynomials are selected using PSO as the nature of this technique that fits this kind of problems. Two-stage optimization problem is formulated. In the first stage, the operating cost is minimized while the minimization of the reactive power sharing error is the objective of the second stage. The universal frequency signal is used along with power consumption costs of the individual sources to construct the frequency droop relations. In the Second stage,

the LFA of the microgrid is used to construct the voltage droop relations that takes into consideration all loading conditions. Moreover, a method is suggested to check and ensure the stability of microgrids with nonlinear droop control. Through simulation and experimental studies, the proposed method was found to be very effective in shaping the droop relations that minimize the operating cost and achieve effective reactive power sharing.

## REFERENCES

[1] S. S. Venkata, A. Pahwa, R.E. Brown and R. D. Christie, "What future distribution engineers need to learn," *IEEE Trans. on Power Syst.*, vol. 19, no. 1, pp. 17–23, 2004.

[2] A. Seon-Ju, P. Jin-Woo, C. Il-Yop, M. Seung-Il, K. Sang-Hee and N. Soon-Ryul, "Power-Sharing Method of Multiple Distributed Generators Considering Control Modes and Configurations of a Microgrid," *IEEE Trans. on Power De*l., vol. 25, pp. 2007–2016, 2010.

[3] A. G. Tsikalakis and N. D. Hatziargyriou, "Centralized control for optimizing microgrids operation," *IEEE Trans. on Energy Convers.*, vol. 23, no. 1, pp. 241–248, 2008.

[4] F. Katiraei and M. R. Iravani, "Power management strategies for a microgrid with multiple distributed generation units," *IEEE Trans.on Power Syst.*, vol. 21, no. 4, pp. 1821–1831, 2006.

[5]J. P. Lopes , C. Moreira and A. G. Madureira, "Defining control strategies for MicroGrids islanded operation," *IEEE Trans. on Power Syst.*, vol. 21, no. 2, pp. 916–924, 2006.

[6] P. N. Vovos, A. E. Kiprakis, A. R. Wallace and G. P. Harrison, "Centralized and distributed voltage control: Impact on distributed generation penetration," *IEEE Trans. on Power Syst.*, vol. 22, no. 1, pp. 476–483, 2007.

[7] H. Jinwei and W. L. Yun, "An Enhanced Microgrid Load Demand Sharing Strategy," *IEEE Trans. on Power Electron.*, vol. 27, no. 9, pp. 3984–3995, 2012.

[8] D. Singh and K. S. Verma, "Multiobjective optimization for DG planning with load models", *IEEE Trans. Power Syst.*, vol. 24, pp. 427–436, 2009.

[9]K. D. Brabandere, B. Bolsens, J. V. D. Keybus, A. Woyte, J. Driesen and R. Belmans, "A voltage and frequency droop control method for parallel inverters," *IEEE Trans. on Power Electron.*, vol. 22, no. 4, pp. 1107–1115, 2007.

[10] T. Senjyu, Y. Miyazato, A. Yona, N. Urasaki and T. Funabashi, "Optimal distribution voltage control and coordination with distributed generation," *IEEE Trans. Power Del.*, vol. 23, no. 2, pp. 1236–1242, 2008.

[11] T. W. Eberly and R. C. Schaefer, "Voltage versus VAr/power-factor regulation on synchronous generators," *IEEE Trans. on Ind. Appl.*, vol. 38, no. 6, pp. 1682–1687, 2002.

[12]C. A. Hernandez-Aramburo, T. C. Green, and N. Mugniot, "Fuel consumption minimization of a microgrid, " *IEEE Trans. Ind. Appl.*, vol.41, no.3, pp. 673-681, May-Jun. 2005.

[13] G. Celli, E. Ghiani, S. Mocci and F. Pilo, "A multiobjective evolutionary algorithm for the sizing and siting of distributed generation," *IEEE Trans. on Power Syst.*, vol. 20, pp. 750–757, 2005.

[14] L. Wang and C. Singh, "Reliability-constrained optimum placement of reclosers and distributed generators in distribution networks using an ant colony system algorithm," *IEEE Trans. Syst., Man, Cybern.*, Part C: Applicat. Rev., vol. 38, no. 6, pp. 757–764, 2008.

[15] Y. d. Valle, G. K. Venayagamoorthy, S. Mohagheghi, J. C. Hernandez and R. G. Harley, "Particle swarm optimization: Basic concepts, variants and applications in power systems," *IEEE Trans. E Comp.*, vol. 12, pp. 171–195, 2008.

[16] J. Kennedy and R. Eberhart, "Particle swarm optimization," *Proc. of IEEE Int. Conf. Neur. Net.*, vol. IV, pp. 1942–1948, 1995.

[17] A. Elrayyah, Y. Sozer and M. Elbuluk, "A Novel Load Flow Analysis for Particle-Swarm Optimized Microgrid Power Sharing," *IEEE Appl. Pow. Electron. Conf. and Expo. (APEC)*, pp. 297–302, 2013.

[18] M. Z. Kamh and R. Iravani, "Unbalanced model and power flow analysis of microgrids and active distribution systems," *IEEE Trans. Power Del.*, vol. 25, no. 4, pp. 2851–2858, 2010.

[19] J. A. Martinez , F. De Leoacute , A. Mehrizi-Sani , M. H. Nehrir , C. Wang and V. Dinavahi, "Tools for analysis and design of distributed resources—Part II: Tools for planning, analysis and design of distribution networks with distributed resources," *IEEE Trans. Power Del*, vol. 26, no. 3, pp. 1697–1705, 2011.

[20] N. Pogaku, M. Prodanovic and T. Green, "Modeling, analysis and testing of autonomous operation of an inverter-based microgrid," *IEEE Trans. Power Electron.*, vol. 22, no. 2, pp. 613–625, 2007.

[21] D. Liberzon and A. S. Morse, "Basic problems in stability and design of switched systems," *IEEE Cont. Syst. Mag.*, vol. 19, pp. 59–70, October 1999.

[22] Y. A.-R. I. Mohamed and E. F. El-Saadany,"Adaptive decentralized droop controller to preserve power sharing stability of paralleled inverters in distributed generation microgrids," *IEEE Trans. Power Electron.*, vol. 23, pp.2806–2816, 2008.

[23] F. Katiraei, M. R. Iravani and P. W. Lehn,"Small-signal dynamic model of a microgrid including conventional and electronically interfaced distributed resources," *IET Gen. Trans. Dist.*, vol. 1, pp.369–378, 2007.